# Performance Improvement of Wind Turbine Driven Induction Generator System

Kanungo Barada Mohanty
Electrical Engineering Department, National Institute of Technology, Rourkela-769008, India
E-mail: kbmohanty@nitrkl.ac.in

***Abstract*- A variable speed wind energy conversion system, with fuzzy control for efficiency optimization and performance enhancement, is discussed in this paper. A squirrel cage induction generator driven by a vertical axis wind turbine feeds the power to a utility grid through two double side pulse width modulated converter system. The generation control system uses three fuzzy controllers. The first fuzzy controller tracks the generator speed with the wind velocity to extract maximum power. The second fuzzy controller programs machine flux for light load efficiency improvement. The third fuzzy controller provides robust speed control against wind vortex and turbine oscillatory torque. The performance of the fuzzy controlled variable speed wind energy conversion system is evaluated through simulation study in MATLAB. Closed loop speed response of the generator with fuzzy controller show fast speed response can be obtained with well designed fuzzy controller.**

## I. INTRODUCTION

The global electrical energy consumption is rising and there is steady increase of the demand on power generation. The existing conventional energy sources are depleting. So, alternative energy source investment is becoming more important these days. Wind electrical power systems are recently getting lot of attention, because they are most cost competitive, environmentally clean and safe renewable source. Of course, the main drawback of wind power is that its availability is somewhat statistical in nature. So it must be supplemented by additional sources to supply the demand curve. In the most preliminary type of wind electrical power system, a fixed speed wind turbine drives an induction generator, directly connected the grid. This system has a number of drawbacks, however. The reactive power and, therefore, the grid voltage level cannot be controlled; the blade rotation causes power and voltage variations [1].

Most of these drawbacks are avoided, when variable-speed wind turbines are used. The power production of variable speed turbines is higher than for fixed speed turbines, as they can rotate at the optimal rotational speed for each wind speed. Noise at low wind speeds is reduced. Other advantages of variable speed wind turbines are reduced mechanical stresses, reduced torque and power pulsations, and improved power quality [2].

The disadvantage of the variable speed turbine is a more complex electrical system, requiring power electronic converters to make the variable speed operation possible. But, the evolution of power semiconductors and variable frequency drive technology has aided the acceptance of variable speed wind generation systems. In spite of additional cost of converters and control, the total energy capture in a variable-speed wind turbine system is larger and therefore the lifecycle cost is lower than with fixed speed system.

The advantages of cage induction machines are well known. These machines are relatively inexpensive, robust, and require low maintenance. When induction machines are operated using vector control techniques, fast dynamic response and accurate torque control are obtained. All of these characteristics are advantageous in variable speed wind energy conversion systems (WECS). Squirrel cage generators with shunt passive or active VAR (volt ampere reactive) generators was proposed in [3], which generate constant frequency power through a diode rectifier and line commutated thyristor inverter. Operation of several self excited induction generators connected to a common bus is analyzed in [4]. The control systems for the operation of indirect rotor flux oriented vector controlled induction machines for variable speed wind energy applications are discussed in [5]-[7]. Sensorless vector control scheme suitable to operate cage induction generator is discussed in [5]. In [6] cage induction machine is considered and a fuzzy control system is used to drive the WECS to the point of maximum energy capture for a given wind velocity. The induction machine is connected to the utility using back-to-back converters.

In this paper a variable speed wind turbine driven squirrel cage induction generator system with two double sided PWM converters is described. Fuzzy control is used to optimize efficiency and enhance performance. The control algorithms are evaluated by MATLAB simulation study.

## II. THE WIND ELECTRICAL GENERATION SYSTEM

### *A. Converter System*

A wind turbine is coupled to the shaft of a squirrel cage induction generator through a speed up gear, which is used to convert the low speed of wind turbine rotor to the high speed of induction generator. The induction generator is then connected to two double side PWM IGBT converters. The generation system feeds power to a utility grid through the converter systems. Some of the features of this system are detailed below.

- Line side power factor is unity with no harmonic current injection.
- Rectifier can generate programmable excitation for the machine.

- Continuous power generation from zero to highest turbine speed is possible.
- Power can flow in either direction permitting the generator to run as a motor for start-up.
- Autonomous operation is possible either with the help of start up capacitor or dc link battery, though present control system is specific for utility connection.

### B. Turbine Characteristics

There are two types of turbines: vertical axis and horizontal axis [7]. A vertical axis turbine does not require any special yaw mechanism, as it need not be oriented with wind direction. The generator is mounted at ground level allowing easier servicing. The system has less weight and lower tower cost. Efficiency of vertical axis Darrieus rotor is slightly less but close to that of horizontal axis propeller type rotor. It is therefore preferred for high power output. The aerodynamic torque of vertical axis Darrieus type turbine is given by [6, 7]:

$$T_m = 0.5\ \rho \pi\ R^3 V_w^2 C_p / \lambda \qquad (1)$$

Where, $C_P$ = Turbine power coefficient,

$\lambda$ = Tip Speed Ratio (TSR), $\rho$ = air density,

R =Turbine radius, $V_w$ = free stream wind velocity,

Turbine power coefficient ($C_P$) is a figure of merit and is defined as the ratio of output power from wind turbine to the available input free stream wind power. Tip speed ratio ($\lambda$) is defined as the ratio of turbine speed at the tip of the blade to the free stream wind speed. $C_P$ is a non linear function of tip speed ratio. The oscillatory torque of the turbine is more dominant at the first, second and fourth harmonics of fundamental turbine angular velocity is given by [6]:

$$T_{osc} = T_m[A.\cos(\omega t) + B.\cos(2\omega t) + C.\cos(4\omega t)] \qquad (2)$$

where, $\omega$ = angular speed of turbine rotor.

### C. Control System

The control block diagram of the wind generation system is shown in Fig. 1. The variable frequency and variable voltage power generated by the machine is rectified and pumped to dc link by IGBT SPWM converter-1, that also supplies lagging excitation current to the machine. The dc link power is fed to utility grid at unity power factor through IGBT SPWM converter-2. The line power factor can be controlled by means of active VAR compensator. The generator speed is controlled by indirect vector control with torque control in its inner loop. Slip speed is generated from q-axis stator current, $i_{qs}$ obtained from the torque controller. Slip speed is added with rotor speed and integrated to synthesize the unit vectors (UV). The line side converter-2 is also vector controlled, using direct vector control. The line voltages and currents are sensed and real power ($P_l$) and reactive power ($Q_l$) are determined to generate unit vectors (UV), $\cos\phi$ and $\sin\phi$. Synchronous current control is used to generate PWM pulses for both the converters. The output line power $P_o$ is controlled to control the dc link voltage $V_d$. Since an increase of line power causes a decrease of dc link voltage, the voltage loop error polarity has been inverted. The insertion of filter inductance $L_s$ creates some coupling effect which is eliminated by a decoupling in the synchronous current control loop. The system uses three fuzzy controllers, as explained in the next section.

## III. FUZZY LOGIC CONTROLLERS

### A. Generator Speed Tracking Controller, FLC-1

For a particular wind velocity, function of FLC-1 is to search the generator speed until the system settles down at the maximum power output condition.

As shown in Fig. 2, for wind velocity $V_{w4}$, the output power is at point-A if the generator speed is $\omega_{r1}$. The FLC-1 alters the speed in steps until it reaches the value $\omega_{r2}$, where the output power is maximum at point-B. If the wind velocity increases to $V_{w2}$, the output power will jump to point-D, and then FLC-1 will bring the operating point to E by searching the speed to $\omega_{r4}$. Similar is the case with decrease in wind velocity. With a change in speed, $\Delta\omega_r$ the corresponding change in output power, $\Delta P_0$ is estimated. Using $\Delta P_0$ and last value of $\Delta\omega_r^*$, i.e., $L\Delta\omega_r^*$ as inputs, FLC-1 generates the required change in speed command, $\Delta\omega_r^*$. The wind vortex and torque ripple can lead the search to be trapped in a local minimum. So the output is added to some amount of $L\Delta\omega_r^*$. The controller operates on a per-unit basis so that the response is insensitive to system variables and the algorithm is universal to any system. The scale factors $K_{P_0}$ and $K_{\omega_r}$, are generated as a function of generator speed ($\omega_r$) so that the control becomes somewhat insensitive to speed variation. The scale factor expressions are given as:

$$K_{P_0} = a_1\ \omega_r \qquad (3)$$

$$K_{\omega_r} = a_2\ \omega_r \qquad (4)$$

Where, $a_1$ and $a_2$ are the constant coefficients obtained from simulation trials.

The asymmetrical triangular membership functions as shown in Fig. 3 are used, because they give more sensitivity as the variables approach zero value. The centroid method is used for defuzzification.

The rule matrix for FLC-1 is given in Table-I. A typical rule of FLC-1 can be read as follows: "If $\Delta P_0$ is PM (positive medium) AND $L\Delta\omega_r^*$ is P (positive), THEN $\Delta\omega_r^*$ is PM (positive medium)."

### B. Generator Flux Controller, FLC-2

The function of FLC-2 is to program the machine rotor flux for light load efficiency improvement. The system output power, $P_o(k)$ is sampled and compared with the previous value, $P_o(k-1)$ to determine the increment $\Delta P_o$. The last excitation current change, $L\Delta i_{ds}^*$ is also considered as the second input. On these bases, the command excitation current, $i_{ds}^*$ is generated from fuzzy controller FLC-2.

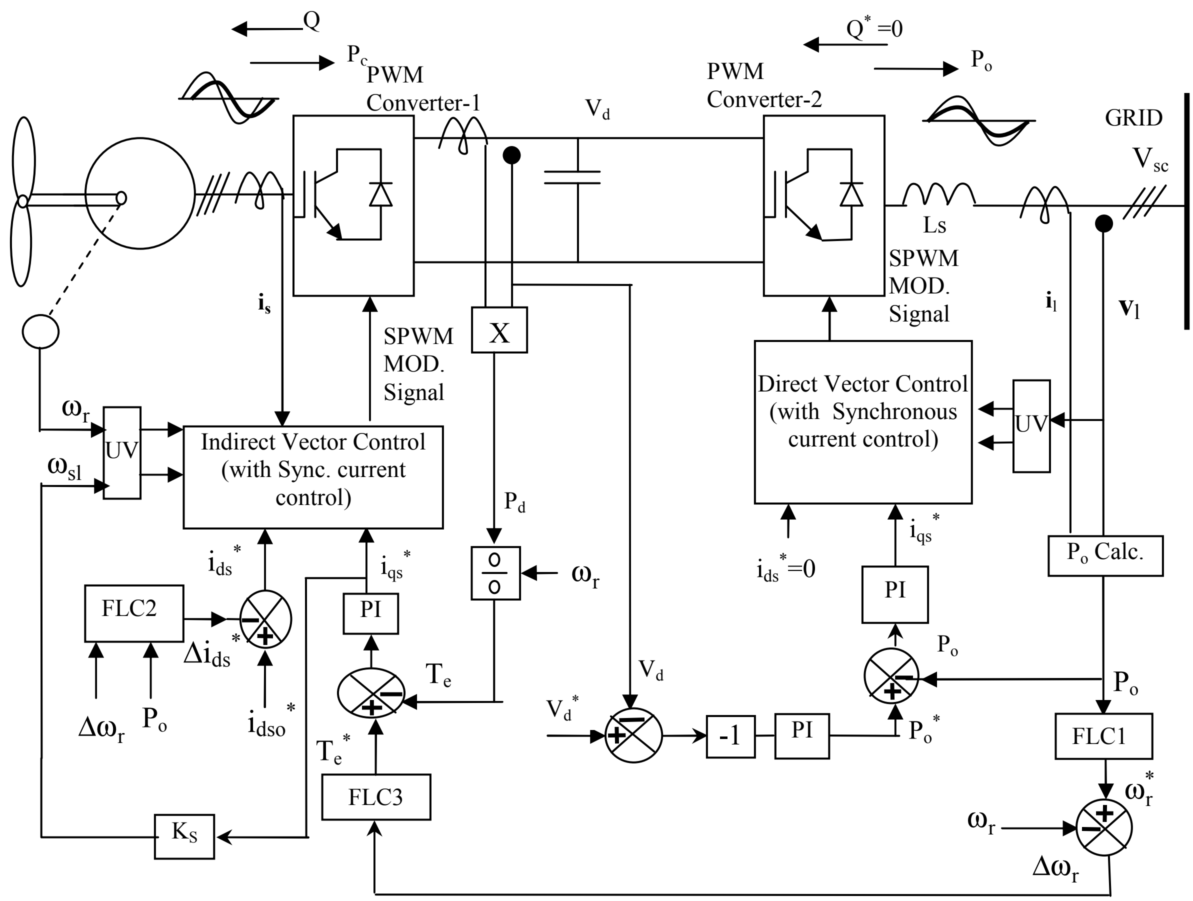


Fig. 1. Block diagram of wind generation system with fuzzy control

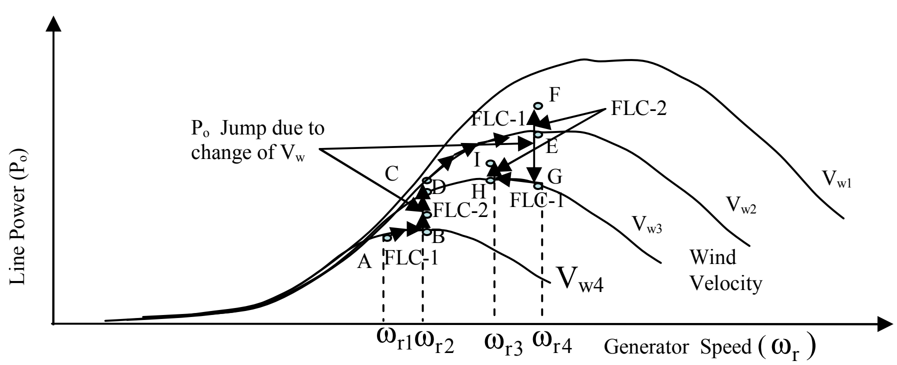


Fig. 2. Maximization of line power through fuzzy controllers, FLC-1 and FLC-2

Adjustable gains $K_P$ and $K_{i_{ds}}$, obtained from simulation trials, are used convert the actual variables to normalized inputs of FLC-2.

$$K_P = a\,\omega_r + b \tag{5}$$

$$K_{i_{ds}} = c_1\omega_r - c_2 i_{qs} + c_3 \tag{6}$$

Where a, b, $c_1$, $c_2$, and $c_3$ are coefficients derived from simulation trials. Asymmetrical triangular membership functions as shown in Fig. 4 are used for the input and output variables. The rule matrix for FLC-2 is given in Table-II. A typical rule can be read as follows: "If $\Delta P_o(k)$ is PM (positive medium) AND $L\Delta i_{ds}^*$ is P (positive), THEN $\Delta i_{ds}^*$ is PS (positive small)."

*C. Closed Loop Speed Controller, FLC -3*

The speed loop error, $E\omega_r$ and change in error $\Delta E\omega_r$ are converted to per-unit values, and processed through fuzzy control, whose rule base is given in Table-III to produce the generator torque component of current, $\Delta i_{qs}^*$. It is to be noted here that while fuzzy controllers FLC-1 and FLC-2 operate in sequence at steady wind velocity, FLC-3 is always active during system operation. The membership functions are same for both the inputs and the output, and are shown in Fig. 5.

TABLE I
RULE MATRIX FOR FLC-1

| $L\Delta\omega_r^*$ / $\Delta P_0$ | P | ZE | N |
|---|---|---|---|
| NVB | NVB | NVB | PVB |
| NB | NB | NVB | PB |
| NM | NM | NB | PM |
| NS | NS | NM | PS |
| ZE | ZE | ZE | ZE |
| PS | PS | PM | NS |
| PM | PM | PB | NM |
| PB | PB | PVB | NB |
| PVB | PVB | PVB | NVB |

TABLE II
RULE MATRIX FOR FLC-2

| $L\Delta i_{ds}$*(pu) / $\Delta P_{0\,(k)}$ | N | P |
|---|---|---|
| PB | NM | PM |
| PM | NS | PS |
| PS | NS | PS |
| ZE | ZE | ZE |
| NS | PS | NS |
| NM | PM | NM |
| NB | PB | NB |

TABLE III
RULE MATRIX FOR FLC-3

| $E\omega_r$(pu) / $\Delta E\omega r$ | NVL | NL | NM | NS | ZE | PS | PM | PL | PVL |
|---|---|---|---|---|---|---|---|---|---|
| NVL | | | | | NVL | NL | NM | NS | ZE |
| NL | | | | | NL | NM | NS | ZE | PS |
| NM | | | | NL | NM | NS | ZE | PS | PM |
| NS | | | NL | NM | NS | ZE | PS | PM | PL |
| ZE | | NL | NM | NS | ZE | PS | PM | PL | |
| PS | NL | NM | NS | ZE | PS | PM | PL | | |
| PM | NM | NS | ZE | PS | PM | PL | | | |
| PL | NS | ZE | PS | PM | PL | | | | |
| PVL | ZE | PS | PM | PL | PVL | | | | |

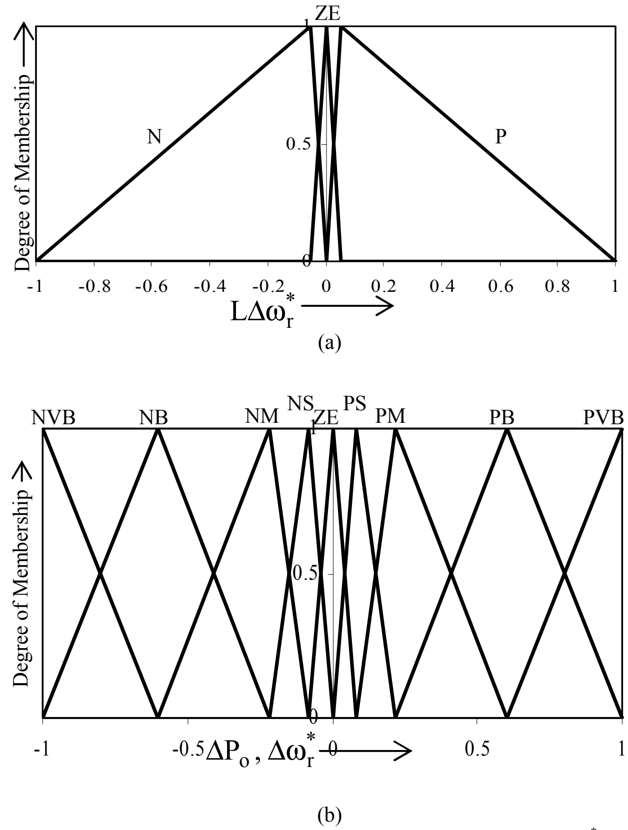


Fig. 3. Membership functions for fuzzy controller FLC-1: (a) $L\Delta\omega_r^*$ (b) $\Delta P_o$ and $\Delta\omega_r^*$

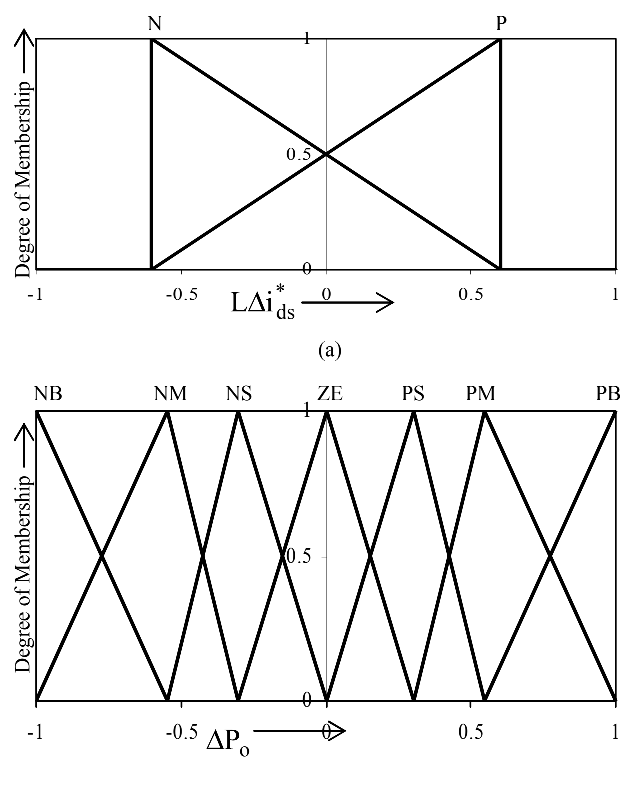

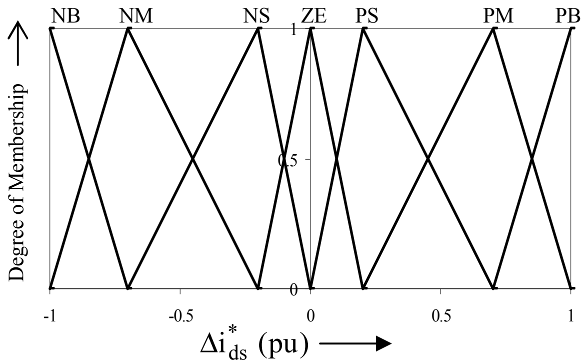


(c)

Fig. 4. Membership functions for fuzzy controller FLC-2 (a) $L\Delta i_{ds}^*$ (b) $\Delta P_o$ (c) $\Delta i_{ds}^*$

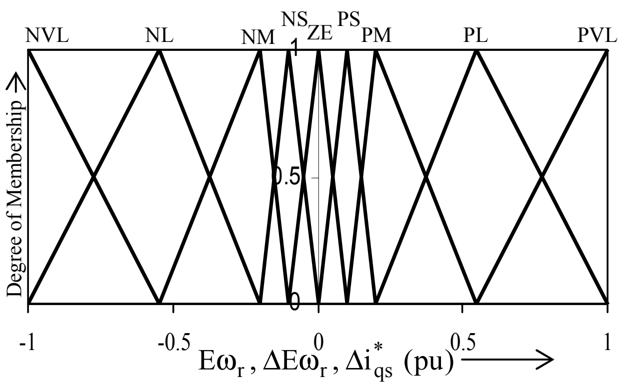


Fig. 5. Membership functions for fuzzy controller FLC-3 ($E\omega_r$, $\Delta E\omega_r$ and $\Delta i_{qs}^*$)

## IV. Results And Discussions

A wind generation system, whose specifications and parameters are given in Table IV, is simulated in MATLAB. The closed loop simulation of the turbine and system model with the control strategies shown in Fig.1, was carried out to evaluate system performance.

TABLE IV
MACHINE, TURBINE AND SYSTEM PARAMETERS

| |
|---|
| **Induction Generator**: 3.5 kW, 230V, 13.4A, 4 pole |
| Stator Resistance = 0.37Ω, Rotor Resistance = 0.436 Ω |
| Stator (rotor) leakage inductance, $L_{ls}$ ($L_{lr}$) = 2.13 mH |
| Magnetizing inductance, $L_m$ = 62.77 mH |
| **Turbine Parameters**: $\eta_g$ = 5.7, A= 0.015, B=0.03, C= 0.015 |
| **System parameters**: Series inductance = 500 μH |
| Line side voltage = 220 V, DC link voltage = 300 V |

### *A. Turbine and System Model Simulation:*

The characteristics of the wind turbine is shown in Fig.6. Power coefficient, $C_p$ is a nonlinear function of tip speed ratio, $\lambda$ and obtained by polynomial curve fitting. The turbine developed torque versus generator speed, for three different wind velocities (6m/s, 8m/s, 10m/s) are shown in Fig.7. The turbine oscillatory torque is ignored in the simulation result for simplicity. For a particular generator speed, if the wind velocity increases, its corresponding turbine torque also increases. Turbine power, which is the product of torque and speed, and the power output at the ac line are also same in nature as the turbine torque.

### *B. Closed Loop Simulation:*

A wind velocity, as shown in Fig.8 is taken as the input for obtaining closed loop response of the wind generation system. Here the turbine is modeled with aerodynamic torque($T_m$) and turbine oscillatory torque ($T_{OSC}$). Some turbulence is also added with the wind velocity to verify the robustness of FLC-3. With this wind velocity, the generator speed, which is response of fuzzy controller FLC-1 is shown in Fig.9. The flux component of the current, which is the response of FLC2 is shown in Fig.10. The output power is shown in Fig.11.

FLC-1 tracks the generator speed with the change in wind velocity to extract maximum power. So, as the wind velocity increases, generator speed also increases due to FLC-1, and the corresponding line output power also increases when the interval FLC-1 is active. Similar is the case for the decrease in wind velocity.

FLC-2 reduces the generator rotor flux for light load efficiency improvement. As FLC-2 reduces the flux component of current, $i_{ds}$ the core loss of machine decreases. On the other hand torque component of current $i_{qs}$ increases, which in turn increases the copper loss of the machine. However, the total system loss i.e., machine and converter loss decrease, resulting in an increase of total generated or output power $P_o$. That is observed in Fig. 11. The increase in output power $P_o$ due to FLC-2, is shown as $\Delta P_o$. Efficiency is improved by about 4% due to this.

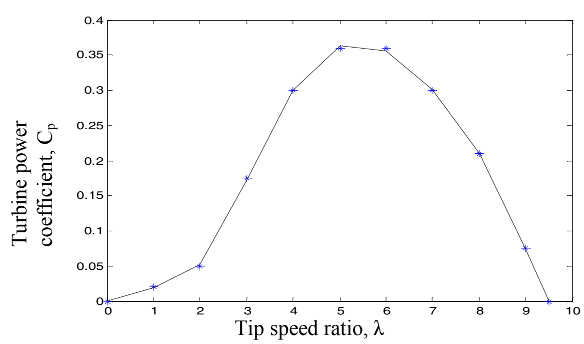


Fig. 6. Turbine power coefficient, $C_p$ as a function of TSR, $\lambda$

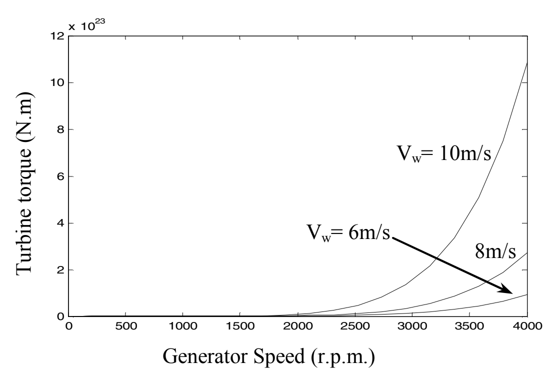


Fig. 7. Turbine torque as a function of generator speed for different wind velocities

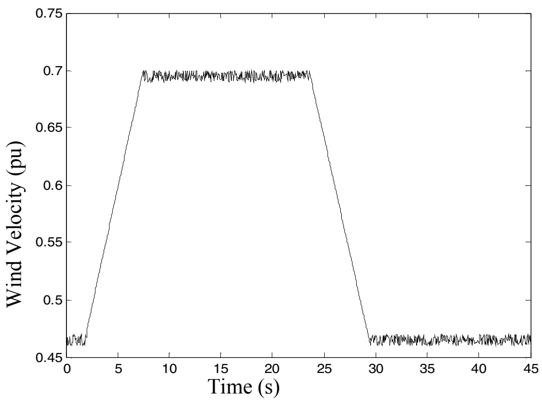


Fig. 8. Wind velocity as a function of time

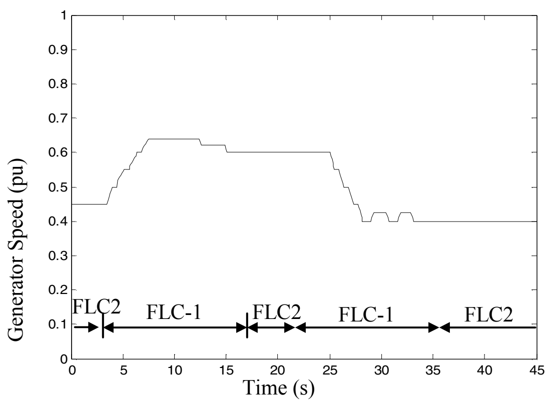


Fig. 9. Generator speed as a function of time

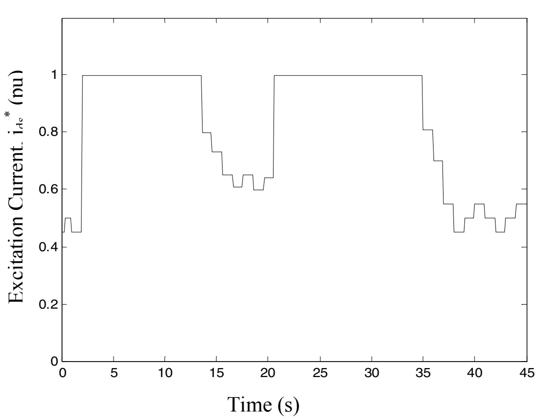


Fig. 10. Flux Component of current as a function of time

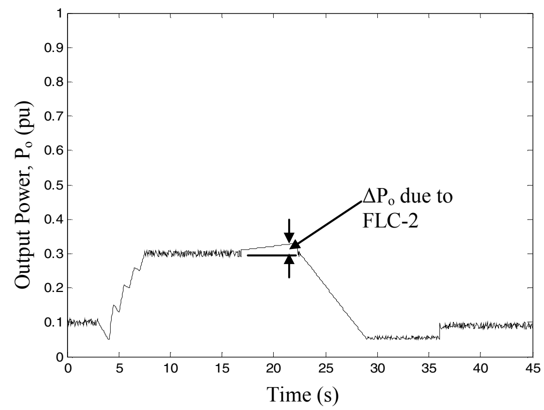


Fig. 11. Output power as a function of time

## V. CONCLUSION

The fuzzy logic based variable speed cage machine wind generation system is analyzed. The control system performance is evaluated through MATLAB simulation. Test results show that there is increase in power output due to the fuzzy controllers FLC-1 and FLC-2. FLC-1 increases the power output by optimizing the generator speed for each wind speed. FLC-2 reduces the core loss, and hence the total loss at light load conditions by adjusting the flux. Efficiency is improved by about 4% due to this. Results also show that FLC-3 gives fast speed response of the closed loop generator system. It is established from the study that the system has more power output, better efficiency and fast response. Thus the performance of the system is better compared to that of conventional system.

## REFERENCES


[1] G. Saccomando, J. Svensson, and A. Sannino, "Improving voltage disturbance rejection for variable speed wind turbines," *IEEE Trans. Egy. Conv.*, vol. 17, no. 3, pp. 422-428, Sep 2002.

[2] J. Morren, and S. W. H. de Hann, "Ridethrough of wind turbines with doubly-fed induction generator during a voltage dip," *IEEE Trans. Egy. Conv.*, vol. 20, no. 2, pp. 435-441, Jun 2005.

[3] C. V. Nayar, and J. H. Bundell, "Output power controller for a wind driven induction generator," *IEEE Trans. Aerospace Electronic Systems*, vol. 23, pp. 388-401, May 1987.

[4] C. Chakraborty, S. N. Bhadra, and A. K. Chattopadhyay, "Analysis of parallel operated self excited induction generators," *IEEE Trans. Egy. Conv.*, vol. 14, no. 2, pp. 209-216, Jun 1999.

[5] R. Cardenas, and R. Pena, "Sensorless vector control of induction machines for variable speed wind energy applications," *IEEE Trans. Egy. Conv.*, vol. 19, no. 1, pp. 196-205, Mar. 2004.

[6] M. G. Simoes, B. K. Bose, R. J. Spiegel, "Design and performance evaluation of a fuzzy logic based variable speed wind generation system," *IEEE Trans. Ind. Appl.*, vol. 33, no. 4, pp. 956-965, Aug. 1997.

[7] S. N. Bhadra, D. Kastha, and S .Banerjee, *Wind Electrical Systems*, Oxford University Press, New Delhi, 2005.

[8] K. B. Mohanty, "Sensorless control of a linearized induction motor drive," *International Review of Electrical Engineering (IREE)*, vol. 2, no. 3, pp. 386-397, June 2007.